

# Role of north tropical atlantic SST on the ENSO simulated using CMIP3 and CMIP5 models

Yoo-Geun Ham · Jong-Seong Kug

Received: 3 June 2014 / Accepted: 13 February 2015 / Published online: 28 February 2015  
© Springer-Verlag Berlin Heidelberg 2015

**Abstract** In this study, role of North Tropical Atlantic (NTA) SST on the ENSO variability is examined with CMIP3 and CMIP5 simulations. It is found that most climate models involved in CMIP3 and CMIP5 successfully simulate the inverse relationship between NTA SST during the boreal spring and the ENSO during the subsequent boreal winter. The multi-model ensemble (MME) results show the observed westward propagating signals related to NTA SST from the Atlantic to the Pacific along the off-equatorial Pacific ITCZ. However, different from the observational argument, the main mechanism for the NTA to induce the ENSO is likely to be different in the MME. While the observational result exhibits the NTA-induced off-equatorial Rossby waves play a more dominant role in leading the Pacific signal, the equatorial wind over the western Pacific related to the NTA-induced Kelvin wave is likely to be more crucial to lead the Pacific variability. In addition, the amplitude of NTA SST-induced ENSO in the MME tends to be systematically weaker, and the preference for the central Pacific SST anomaly is also weak. These weak signals are distinctly improved in a model that simulates two types of El Niño events independently. That the strength of the NTA effect to the Pacific can be affected by the seasonal distribution of climatological precipitation is also discussed. Additionally, the strength of the NTA effect tends to be stronger when the model simulates phase locking of ENSO reasonably.

**Keywords** ENSO · North Tropical Atlantic · Climate models

## 1 Introduction

It is well known that there is a strong co-variability and interaction among the tropical oceanic basins. On the one hand, many studies have reported the influence of the El Niño-Southern Oscillation (ENSO) on the Atlantic ocean (Covey and Hastenrath 1978; Curtis and Hastenrath 1995; Enfield and Mayer 1997; Klein et al. 1999; Alexander and Scott 2002; Illig and Dewitte 2006) and Indian ocean sea surface temperature (SST) with few months lag (Klein et al. 1999; Wu and Kirtman 2004; Kug et al. 2004). The modulation of the Walker Circulation and related surface wind and heat flux change is one of key mechanisms in regulating Indian Ocean and Atlantic SST variability during the ENSO.

On the other hand, opposite to the dominant role of Pacific SST variability on the other ocean basins, recent studies have emphasized that tropical SST variability outside of the Pacific can modulate ENSO variability. Several studies have examined the role of the Indian Ocean in the ENSO (Wu and Kirtman 2004; Kug et al. 2005; Kug and Kang 2006; Izumo et al. 2010; Ohba and Watanabe 2012; Kug and Ham 2012). In particular, Kug and Kang (2006) suggested that the Indian Ocean warming concurrent with El Niño events tends to lead to a faster transition of the El Niño to the La Niña, which might lead to the biennial tendency of the ENSO. The additional low-level easterly in the western Pacific due to the Indian Ocean warming during the El Niño helps a rapid termination of El Niño by generating upwelling Kelvin waves.

Additionally, studies about the inter-basin interaction between the Atlantic and Pacific SST variability have

---

Y.-G. Ham  
Faculty of Earth Systems and Environmental Sciences, Chonnam National University, Gwangju, South Korea

J.-S. Kug (✉)  
School of Earth Science and Engineering, Pohang University of Science and Technology (POSTECH), Pohang, South Korea  
e-mail: jskug@postech.ac.kr

increased since the recognition of equatorial SST variability over the Atlantic, which is often called the “Atlantic Niño” due to its similar ocean-atmospheric coupled characteristics with the El Niño over the Pacific (Merle et al. 1980; Servain et al. 1982; Keenlyside and Latif 2007). After these findings, several studies suggested the role of equatorial Atlantic SST on ENSO (Dommenges et al. 2006; Dong et al. 2006; Jansen et al. 2009; Rodríguez-Fonseca et al. 2009; Ding et al. 2012; Frauen and Dommenges 2012). According to these studies, the positive phase of Atlantic Niño during the boreal summer season can lead to a La Niña signal during the subsequent winter season through strengthening of the Walker circulation with an ascending branch over the Atlantic and a descending branch over the western Pacific. Then, the low-level easterly over the western Pacific shifts the equatorial thermocline over the equatorial Pacific, which can lead to the development of a La Niña (Rodríguez-Fonseca et al. 2009).

On the other hand, Ham et al. (2013a) suggested that the North Tropical Atlantic (NTA) SST play a role in modulating the Pacific SST variability. That is, the NTA cooling during the boreal spring season induces the El Niño signal after two or three seasons, indicating that there is a lagged negative relationship between NTA SST and the ENSO. According to their study, once the NTA cooling is induced, the decrease in local precipitation generates low-level anticyclonic flow over the west of the decreased precipitation. The southerly at the western edge of the low-level anticyclone is located over the off-equatorial far eastern Pacific, and acts to induce a local SST warming due to the reduced wind speed and warm and wet moist energy transport. This SST and the related positive precipitation anomalies over the eastern Pacific generate low-level cyclonic flow over the central Pacific, which also leads to an equatorial westerly over the western-central Pacific. This equatorial westerly excites a downwelling Kelvin wave, leading to an El Niño signal over the central Pacific during the boreal winter. These processes show slowly westward propagating features from the Atlantic to the western Pacific along the Inter-tropical Convergence Zone (ITCZ), representing the off-equatorial bridge. In addition to the off-equatorial bridge along the Pacific ITCZ, the Kelvin wave response to the NTA SST over the Indian and maritime continent may play some roles in this inter-basin relationship. Ham et al. (2013b) also found that the El Niño case, affected by the NTA SST, is mainly a Warm-Pool (WP) type with the SST action center over the central Pacific (Ashok et al. 2007; Kug et al. 2009; Kao and Yu 2009; Yeh et al. 2014).

The observational analyses are limited in demonstrating the suggested hypothesis due to the sampling issue. Accordingly, Ham et al. (2013a) carried out idealized experiments using a coupled GCM to support the observational hypothesis. Although they showed that both the CMIP3 and CMIP5 model results supported the observational arguments

successfully without any significant differences between two groups, they also pointed out that the response could be model-dependent. Given this, it is valuable to examine the interaction process based on a multi-model framework. This is important for further understanding the physical processes on the dynamic relationship between the two ocean basins. Ham et al. (2013b) also emphasized the impact of the equatorial Pacific SST to the NTA SST can be critical in simulating the right amplitude of moderate El Niño events, which tends to be hard to predict (Hendon et al. 2009; Jeong et al. 2012). This indicates that simulating the right intensity and spatial structure of the response induced by the NTA SST may be a crucial factor in determining the quality of ENSO forecasts. Thus, it is important to investigate in more detail how well the role of NTA SST on Pacific SST is simulated in climate models, and try to understand the possible factors to improve the simulation of this inter-basin relationship.

Given this background, this study will examine how well the observed role of NTA SST on ENSO variability is simulated in the CMIP3 and CMIP5 models. In Sect. 2, descriptions of the observational data and CMIP model outputs used in this study are provided. The overall simulation quality and multi-model ensemble (MME) result about the role of NTA SST on Pacific SST variability will be examined in Sect. 3. Section 4 will cover possible reasons for inter-model differences in the strength of NTA SST responses among climate models. A summary and conclusions are presented in Sect. 5.

## 2 Data

In this study, we used multi-model outputs in CMIP3 and CMIP5. The 21 and 23 CGCM simulations in the pre-industrial simulation in CMIP3 and CMIP5 are also analyzed, respectively. Model references, details of the institutions where the models were run, and integration periods are summarized in Table 1. For the observational data, we used monthly-mean wind, geopotential height, and precipitation from 1980 to 2010, obtained from the Modern ERA Retrospective-analysis for Research and Applications (MERRA, Rienecker et al. 2011). The observed SST data during 1980–2010 are the improved extended reconstructed SST version 3 (ERSST V3) from the National Climate Data Center of the US (Smith et al. 2008). All the data are detrended before analyzing.

## 3 The role of NTA SST on ENSO variability in CMIP models

Ham et al. (2013a) used a partial regression to isolate the ENSO signal in the previous winter season (i.e., the

**Table 1** Description of the models from the CMIP3 and CMIP5 archives

Archive	Modeling group	Model number	CMIP ID	Integration period (years)	
CMIP3	LASG	1	IAP_FGOALS-g1.0	150	
	Météo-France	5	CNRM-CM3	500	
	NOAA/GFDL	6	GFDL-CM2.1	500	
	University of Bonn, KMA	9	MIUB_ECHO-G	340	
	Max-Planck-Institute	10	MPI-ECHAM5	500	
	CSIRO Atmospheric Research	11	CSIRO-Mk3.5	500	
	NOAA/GFDL	15	GFDL-CM2.0	500	
	Hadley Centre/Met Office	17	UKMO-HadCM3	250	
	CCSR, JAMSTEC	21	MIROC3.2_MEDRES	500	
	INGV	23	INGV_ECHAM4	100	
	BCCR	25	BCCR-BCM2.0	250	
	IPSL	27	IPSL-CM4	500	
	CCCMA	29	CCCMA_CGCM_3.1	500	
	CCCMA	30	CCCMA_CGCM_3.1_t63	400	
	Hadley Centre/Met Office	33	UKMO-HadGEM1	230	
	MRI	34	MRI-CGCM2.3.2a	350	
	INM	35	INM-CM3.0	330	
	NCAR	37	NCAR-PCM1	300	
	CSIRO Atmospheric Research	39	CSIRO-Mk3.0	380	
	CCSR, JAMSTEC	42	MIROC3.2_HIRES	100	
	NCAR	43	NCAR-CCSM3.0	230	
	CMIP5	NCAR	2	CCSM4	500
		NASA/GISS	3	GISS-E2-H	480
		NOAA/GFDL	4	GFDL-ESM2 M	500
		LASG	7	FGOALS-g2	500
		CCSR, JAMSTEC	8	MIROC5	670
		NCC	12	NorESM1-M	500
		LASG	13	FGOALS-s2	700
		NASA/GISS	14	GISS-E2-R	850
		Météo-France	16	CNRM-CM5	850
		NOAA/GFDL	18	GFDL-ESM2G	500
		Hadley Centre/Met Office	19	HadGEM2-CC	240
		NOAA/GFDL	20	GFDL-CM3	500
MRI		22	MRI-CGCM3	500	
MPI-M		24	MPI-ESM-LR	1000	
Hadley Centre/Met Office		26	HadGEM2-ES	480	
CCSR, JAMSTEC		28	MIROC4 h	100	
MPI-M		31	MPI-ESM-P	1000	
CCSR, JAMSTEC		32	MIROC-ESM	530	
CSIRO		36	CSIRO-Mk3-6-0	500	
BCCR		38	BCC-CSM1.1	500	
IPSL		40	IPSL-CM5A-MR	1000	
IPSL	41	IPSL-CM5A-LR	1000		
INM	44	INM-CM4	500		

previous DJF season) from the NTA SST (90°W–20°E, 0–15°N) variability during the FMA season. Excluding the previous ENSO signal is to isolate the ENSO response induced by NTA SST from that due to its oscillatory

feature. In this study, we used the CGCM simulation in the same way that the regression onto NTA SST during FMA season is calculated after excluding the ENSO signal of the previous DJF season. To quantify the role of NTA SST on

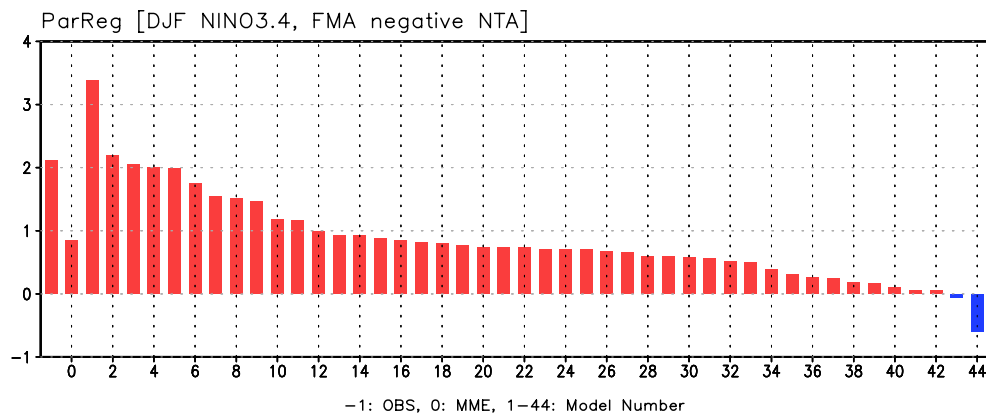


**Fig. 1** The regression coefficient of DJF NINO3.4 SST on the unit change of FMA NTA SST after excluding NINO3.4 SST during the previous DJF season. The number ‘-1’ in x-axis denotes the

observed, 0 denotes the multi-model ensemble (MME) value, and 1–44 denote the climate models within CMIP3 and CMIP5

ENSO variability, Fig. 1 shows the regression coefficient of DJF NINO3.4 SST on the unit change of FMA NTA SST after excluding effect of NINO3.4 SST during the previous DJF season. Note that we multiplied the negative one by the regression coefficient to denote the change of NINO3.4 SST when a negative NTA SST is given. For ease of comparison, the climate models are rearranged in order of the regression coefficient (from high to low).

In the observation, the regression coefficient is slightly above 2 °C. This indicates that the anomalous 1 °C cooling over NTA during FMA is linked to the 2 °C warming over the NINO3.4 region during the subsequent DJF, on average. However, the regression coefficient of the MME is smaller than 1 °C, meaning that the models tend to underestimate the role of NTA SST on ENSO variability. Consistently, the regression coefficients in climate models are systematically smaller than the observed value except two models. There can be several reasons for the weak NTA responses over the Pacific. One of them is the direct response to the NTA SST is realistic, but this signal is not amplified enough due to the weak coupled atmosphere–ocean feedbacks within the Pacific. Kim and Jin (Kim and Jin 2011) showed that the most CMIP models have weaker thermocline and zonal advective feedback to determine the ENSO amplitude. The other possibility is that the direct response to the NTA SST, for example the wind response to the NTA SST, is different in the models. We will investigate which is the case in the later part of this paper in more detail.

However, it is interesting that most models (i.e., 42 of 44 models) simulate positive NINO3.4 values when there is negative NTA SST, indicating that the inverse relationship between NTA SST and subsequent ENSO signal is well simulated in the climate models. We define this regression coefficient as the ‘Strength of NTA-Effect’ (SNE) index to

quantify the strength of NTA SST impacts on the ENSO variability. We will use the SNE index to examine the inter-model differences in the role of NTA SST.

Figure 2 shows the composite of the normalized DJF NINO3.4 index with NTA SST events. The NTA warming (cooling) case is defined when the NTA SST index is larger (smaller) than one (minus one) standard deviation (STD) during the previous FMA season. To exclude the effect of the ENSO signal in the previous year, the composite cases are further confined only when the magnitude of NINO3.4 SST during the previous DJF season is smaller than 0.5 STD. Consistent with the partial regression result, the amplitude of the MME value is smaller than that of the observation, confirming that the climate models tend to underestimate the role of NTA SST on the Pacific variability. Among the total of 44 climate models, 32 models simulated the El Niño after the NTA cooling. On the other hand, only five models simulated the La Niña signal after the NTA cooling, supporting the notion that the NTA cooling can initiate the El Niño during the subsequent winter season. With the NTA warming, 30 climate models (i.e., 68 % of total number of models) simulated a significant La Niña signal, while nine models simulated an El Niño signal after NTA warming.

Interestingly, there is an asymmetry between NTA warming and cooling cases; the amplitude of the El Niño induced by NTA cooling is larger than that of the La Niña induced by NTA warming. This asymmetry is clear in the observations that the NINO3.4 SST is 1.14 after the NTA cooling case, while it is -0.49 after the NTA warming case. It is also supported in the MME, although the asymmetry is likely to be weaker than the observed. The NINO3.4 SST after NTA cooling is 0.34, while that after NTA warming is -0.22. This asymmetry should be examined in further studies.

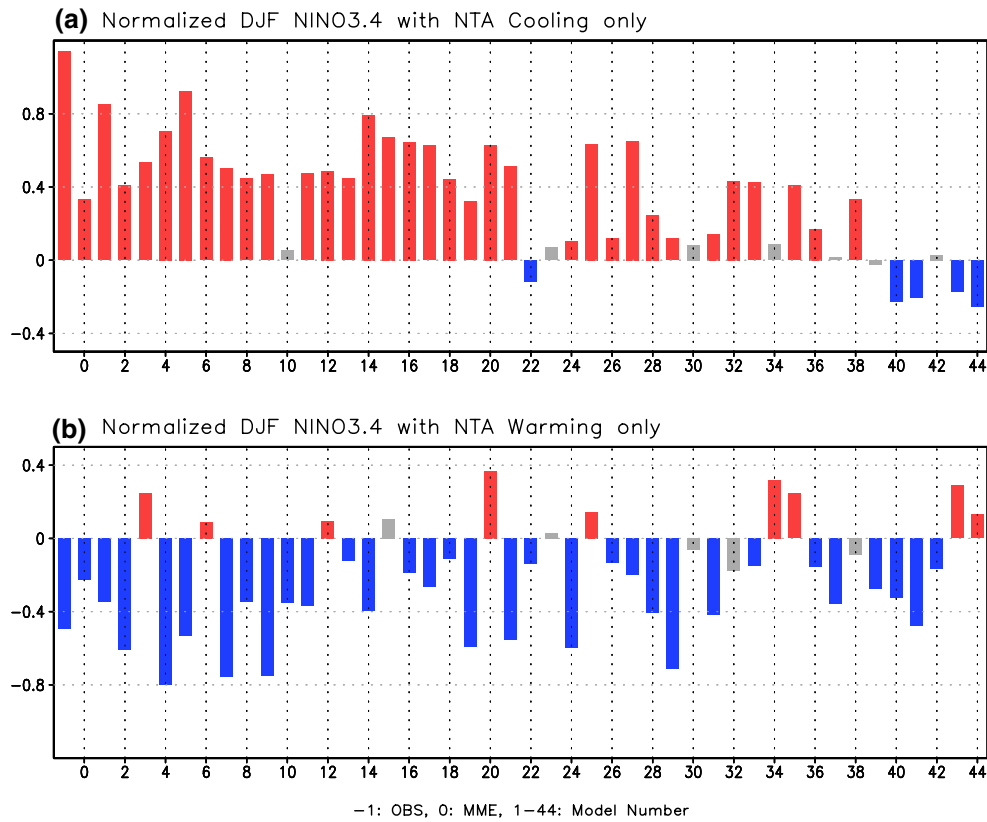


**Fig. 2** The magnitude of NINO3.4 SST during DJF season with significant NTA SST (i.e., larger than 1 standard deviation) during the previous FMA season for use in CMIP3 and CMIP5. Only cases

where the magnitude of NINO3.4 SST during the previous DJF season was smaller than 0.5 standard deviation were selected to exclude the ENSO signal from the previous year

Figures 1 and 2 show that NTA SST is closely correlated with the NINO 3.4 SST about 10 months later by compositing every events in each model. To look at the probabilistic distribution and emphasize the role of NTA as a trigger of ENSO events, Fig. 3 shows the occurrence percentage of El Niño, normal, and La Niña events during the subsequent DJF season when an NTA SST event during the previous FMA season. We used the FMA NTA events only when the amplitude of the Nino3.4 SST during the previous DJF season is <0.5 STD to exclude the impact of previous year’s ENSO signal. As the ENSO event is defined when it is greater 0.5 STD, so that the ratio for El Niño development would be about 30 % (denoted by the black solid line) by assuming a normal distribution, if the NTA SST plays no role. Although the onsets of El Niño and La Niña are largely determined by the residing ocean memories over the tropical Pacific, as the ENSO theories suggest (Jin 1997), the MME result indicates that 45 % of NTA cooling cases lead to subsequent El Niño events, while only 17 % of NTA cooling cases is linked to subsequent La Niña events. That means the most of the models show that NTA cooling leads to a higher chance for El Niño development and lower chance for La Niña development in the subsequent winter.

The opposite is also evident that NTA warming leads to a higher chance for the subsequent La Niña (40 %) than the El Niño (23 %). This indicates that the NTA SST can be an important component in triggering an ENSO event.

One can be curious about how often the El Nino is induced by NTA SST. The occurrence of NTA-warming-induced El Nino is about 7 % of total El Nino events in the MME. In observation, the total number of El Nino events defined as when DJF Nino3.4 is >0.5 STD is 9 from 1980 to 2010, and there was significant amplitude of NTA cooling SST during previous FMA season for 86/87, 94/95, 09/10 El Nino events (Ham et al. 2013b), which indicates 33 % of total El Nino events are induced by the NTA-cooling. This implies that the occurrence ratio of NTA-induced El Nino events is also underestimated in the MME as the amplitude of Nino3.4 SST induced by NTA SST is underestimated.

So far, several lines of the statistical evidences have been provided in a multi-model framework that the NTA SST plays a considerable role in modulating ENSO variability. Thus, it is important to understand which physical processes work for the NTA connection to ENSO in climate models, and to assess whether the state-of-the-art climate models actually simulate the observed physical processes.

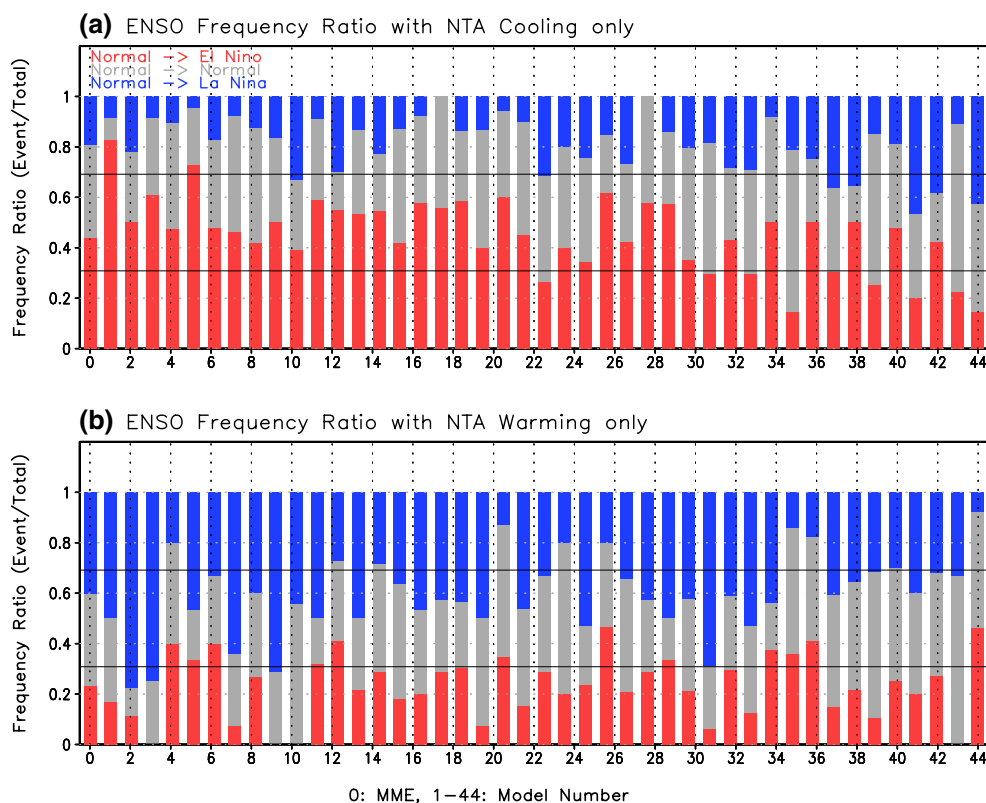


**Fig. 3** **a** The ratio of El Niño, normal, and La Niña events during the following DJF season when the NTA SST cooling during the FMA occurs without an ENSO event. **b** Same as (a), but for the NTA warming case

To address these, Fig. 4 shows the spatial distribution of MME, partial regression of SST, precipitation, and 850 hPa wind vector onto the FMA NTA SST without the effect of NINO3.4 in the previous DJF season, as shown in Figure 1 of Ham et al. (2013a). As shown in left panels of Fig. 4, the observational results showed that the positive NTA SST induced a low-level cyclonic flow over the far eastern Pacific during the MAM season (see Fig. 1 of Ham et al. 2013a). Over the western edge of the low-level cyclonic flow, the northerly induces SST cooling and negative precipitation due to the increased wind speed and cold and dry moist energy from higher latitudes. During the JJA season, it was shown that the magnitude of negative precipitation over the off-equatorial northern Pacific was intensified, and this atmospheric cooling induced the anticyclonic flow over the central-western Pacific. Along this equatorial easterly over the western Pacific related to this anticyclonic flow, the La Niña signal starts to develop from the JJA season. During the SON season, the La Niña signal prevails over the equatorial Pacific through air-sea-coupled feedback.

In the MME, in right panels of Fig. 4, the climate models successfully simulate the low-level cyclonic flow over the far eastern Pacific in the response to the NTA warming during the MAM season. The negative precipitation associated

with the northerly is also well simulated in the MME. During the JJA season, the negative precipitation anomalies are intensified and expanded to the west, and the negative SST anomalies over the eastern Pacific are induced, as in the observed. During the SON season, the anticyclonic flow over the central-eastern Pacific and associated La Niña signal is clearly seen. During the DJF season, the La Niña signal prevails over the equatorial Pacific through air-sea-coupled feedback. This indicates that the MME results are generally consistent with the observed, implying that the climate models tend to simulate the observed role of the NTA SST on the Pacific variability, to some degree.

However, there are also some clear differences between the model simulations and observations. First, the main mechanism for the NTA SST to lead ENSO signal in the MME is likely to be different from the observation. In the MME, while the equatorial easterly during the boreal spring over the Indian Ocean is much robust, the off-equatorial SST signal over the far-eastern Pacific is not clear. That is, the NTA-induced Kelvin wave which propagates to the downstream might be crucial to lead the ENSO signal in the MME, while the observational result exhibits NTA-induced Rossby wave propagates to the upstream is important. In short, the model simulates correct response to

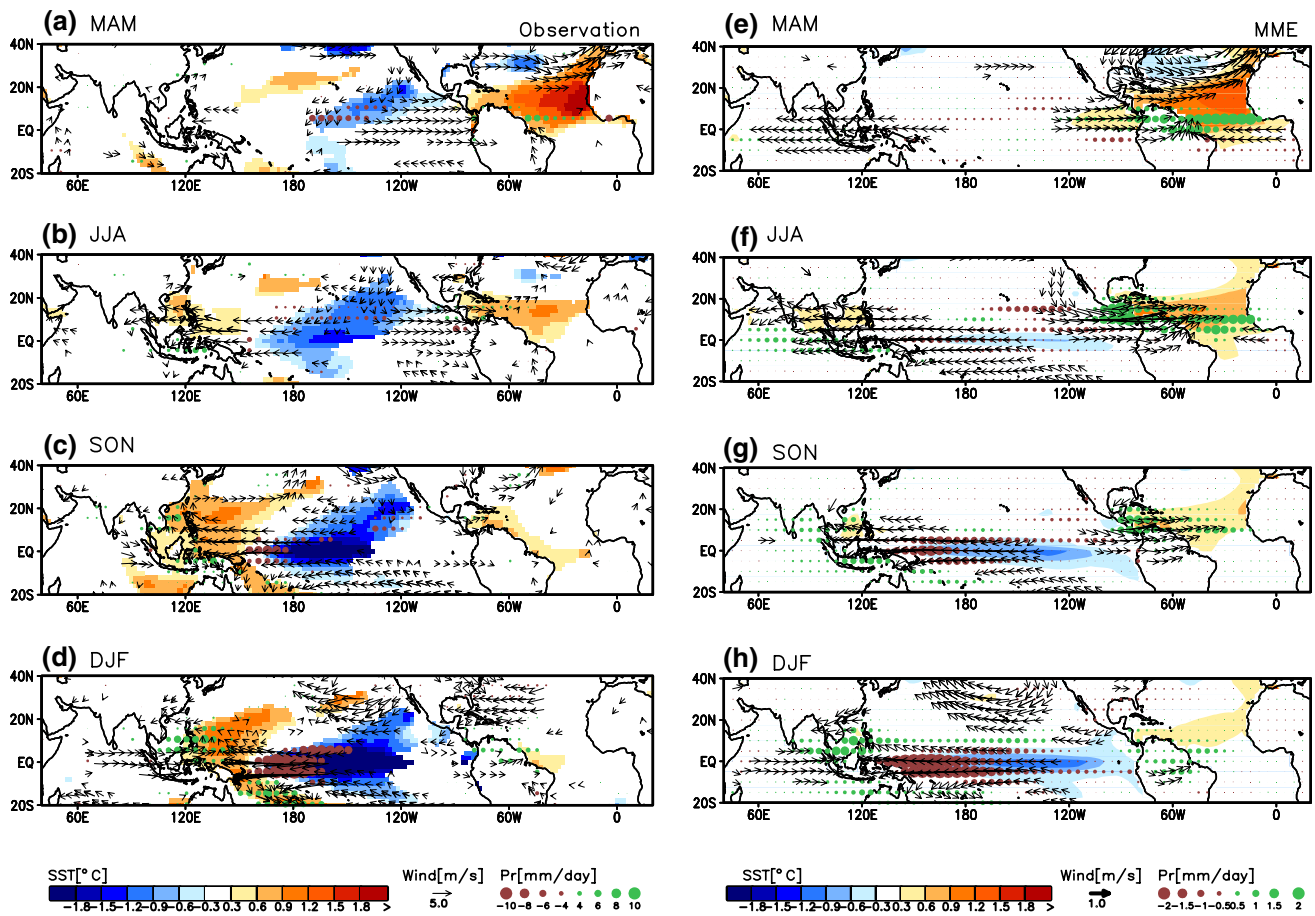


**Fig. 4** The *left panels* show the observational partial regression of SST, precipitation, and wind vector at 850 hPa during the **a** MAM, **b** JJA, **c** SON, and **d** DJF season onto the FMA NTA SST after exclud-

ing the impact of NINO3.4 during previous DJF season. The *right panels* is same as *left panels*, but for the MME

the NTA SST over the Pacific but their underlying mechanisms are different to some extent. This may be related to the underestimation of the NTA SST-induced responses over the Pacific. In addition, the simulated ENSO during SON and DJF has stronger variability over the east of the international dateline, while the observed one is more confined to the west. For example, in the observation, the SST anomalies over the eastern Pacific are near-zero during the SON season [i.e., Fig. 1c in Ham et al. (2013a)], while the MME exhibits strong surface cooling, expanded to the eastern Pacific. That is, the observed NTA-induced ENSO is likely WP-type, while that in MME is difficult to define to the type of ENSO.

However, it is interesting that the low-level wind responses during MAM and JJA exhibits an equatorial easterly over the western Pacific and an equatorial westerly over the eastern Pacific with NTA SST warming. Therefore, over the eastern Pacific, the impact of western Pacific easterly will be weakened due to the local westerly which is the key atmospheric response to suppress the

eastern Pacific SST variability to prefer the development of the WP-type ENSO. These opposite responses between the western Pacific and eastern Pacific are consistent with the observational features. However, the SST suppression related to the westerly over the eastern Pacific is not clear in the model simulation. That is, the local westerly over the eastern Pacific cancels out the local SST cooling by suppressing equatorial upwelling in the observation, but this feature is not clear in the MME.

For example, during the JJA season, there is a negative SST anomaly to the east of 120°W, where there is a local westerly. The relative amplitude of the eastern Pacific westerly, which acts to reduce the SST variability by cancelling the contribution of the western Pacific wind, is quite similar to that of the western Pacific in MME (i.e., ratio of westerly over the equatorial (5°S–5°N) eastern Pacific wind to equatorial easterly over the western-central Pacific is 0.56 in observation, and 1.27 in MME). It means that the cancellation is not clear in the MME, even though the amplitude of westerly wind forcing is greater. This indicates that the

SST response to the local wind over the eastern Pacific is insensitive in the MME, possibly due to weak background upwelling and diffuse thermocline. This weak response of eastern Pacific SST anomalies to the local wind forcing leads to the prevailing response of remote wind forcing over the western Pacific, so that the SST anomalies are greatly extended to the east in the MME, while there is weak SST signal over the eastern Pacific in the observation.

This may lead to the strong co-variability between the central and eastern Pacific SST in the model simulation, which may affect the degree of simulating the two types of El Niño events independently. That is, the independency between the central and eastern Pacific SST would be increased when the SST variability over the eastern Pacific is effectively affected by local wind forcing, because it only affects the eastern Pacific SST. However, when the western Pacific wind prevails in the response of the SST anomalies over the both central and eastern Pacific, it would decrease the independency between the two types of El Niño events. Thus, the weak response to the local wind forcing over the eastern Pacific might cause the deficiency that the climate models tend to simulate a single-type El Niño.

One can also wonder whether the climatological bias can affect to the WP El Niño-type response to the NTA forcing. To examine this aspect, we categorize two groups based on the mean SST. One group is the models whose mean SST over the equatorial central-eastern Pacific (150°E–150°W, 5°S–5°N) is higher than the MME, and the other is mean SST over the central-eastern Pacific is lower than the MME. It is found that the SST response to the NTA forcing is different in some aspect between two groups. In models with warmer mean SST, the La Niña signal reaches 2 °C during the DJF season, while in models with colder mean SST, it is systematically weaker (i.e. less than –1 °C) (not shown). In addition, during the SON season, the center location of La Niña is clearly shifted to the west in models with warmer mean SST. As most climate models suffers cold SST bias, it implies that the models with realistic climatology can simulate somewhat similar NTA remote response.

Other differences include that the MME result shows a connection between NTA SST and Indian Ocean SST. As shown in Fig. 4b, the NTA warming tends to lead to Indian Ocean warming, by reducing monsoonal flow during the boreal summer season. That is related to the easterly Kelvin wave response at the east of the NTA warming. This Kelvin response was not that robust in the observation, unlike that of the MME, implying that the models tend to simulate a stronger equatorial wind response to the NTA SST than the observed. This might enhance the role of NTA SST on the ENSO as the additional Indian Ocean warming can also lead to a La Niña signal during the subsequent winter season (Kug and Kang 2006; Kug et al. 2006a, b; Ohba and Ueda 2007, 2009; Ohba et al. 2010).

In addition to being an effective trigger of the ENSO, it has also been suggested that the NTA SST can lead to a fast phase transition of the ENSO (Dommenges et al. 2006), as some ENSO events accompany NTA SST events (Covey and Hastenrath 1978; Alexander and Scott 2002). To measure the impact of NTA SST on the ENSO transition, we first selected La Niña events that accompany the NTA cooling during the following FMA season. Then, we compared the evolution of La Niña events without NTA cooling. Figure 5 shows the evolution of SST and precipitation anomalies with and without NTA cooling during the La Niña decaying phase. During the MAM season, it is clear that there is NTA cooling in a ‘La Niña + NTA cooling’ composite, as expected. Note that the amplitude of the La Niña over the equatorial Pacific is similar in both composites, while the Indian Ocean cooling is slightly stronger in the ‘La Niña + NTA cooling’ composite. During JJA season, the spatial pattern of SST anomalies is similar in both composites, while the negative SST anomalies over the eastern Pacific are weaker in ‘La Niña + NTA cooling’ composite. During the SON season, there is a positive SST signal over the eastern Pacific in ‘La Niña + NTA cooling,’ indicating the fast phase transition from the La Niña to El Niño, which is shown clearly. However, this El Niño signal is much weaker in the ‘La Niña only’ composite. This difference is still obvious during the DJF season, which shows that NTA SST can lead to a fast transition of the ENSO in the MME.

So far, we have shown that NTA SST can influence the ENSO in two ways: when the NTA SST occurs independently without the ENSO, it can act to trigger the ENSO, and, when NTA cooling is accompanied by La Niña, it plays a role in leading a fast phase transition of the ENSO. Those two arguments are shown separately; however, the physical processes (i.e., NTA as an ENSO trigger, and NTA as a fast ENSO transition mechanism) are basically the same. Figure 6 shows the difference in the 850 hPa zonal wind in ‘La Niña + NTA cooling’ and that in the ‘La Niña only’ composite. The overall wind difference is quite similar to Fig. 4, examining the role of NTA SST without ENSO, indicating that the physical processes are similar.

During the MAM season, there is an easterly over the equatorial far-eastern Pacific, while there is a westerly signal over the equatorial Atlantic and Indian Ocean. This is due to atmospheric cooling over the equatorial Atlantic, related to the negative NTA SST. During the JJA season, the opposite wind response between western and eastern Pacific becomes clear, which is a key response to the NTA SST over the equatorial Pacific. Interestingly, those wind responses are clear even though the Pacific SST signal is quite similar between the two composites (Fig. 5c, d), supporting that those winds are not induced by the Pacific SST. This equatorial westerly over the western Pacific is related



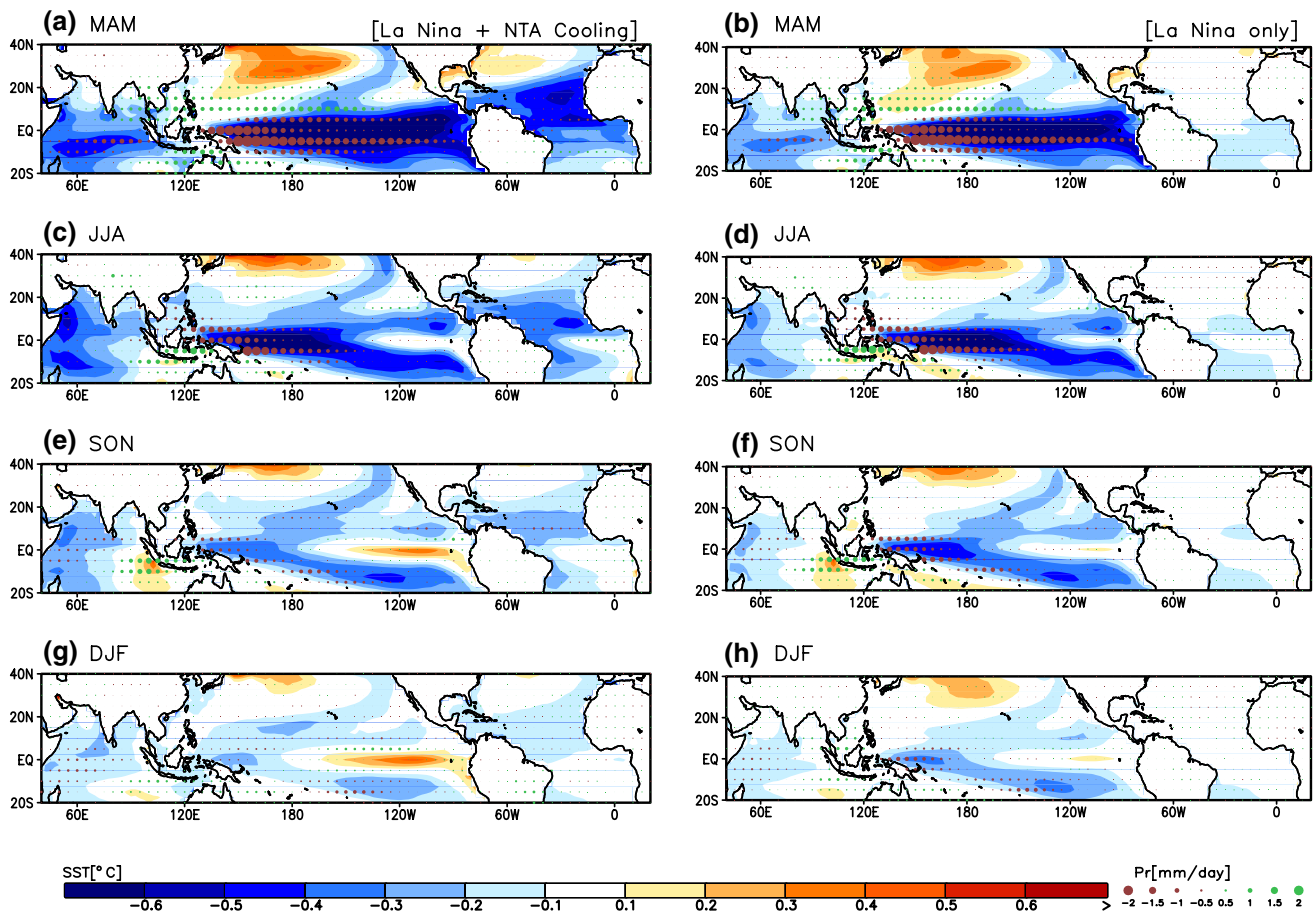


**Fig. 5** The left and right panels show composite of SST and precipitation during **a** MAM, **b** JJA, **c** SON, and **d** DJF seasons after the peak of La Niña events in ‘La Niña + NTA cooling’ and ‘La Niña only’ composites, respectively. The ‘La Niña + NTA cooling’ composite is performed using the La Niña case (i.e., DJF NINO3.4 is

smaller than  $-1$  standard deviation) with significant NTA cooling (i.e., FMA NTA SST is smaller than  $-1$  standard deviation), while the ‘La Niña only’ composite is when FMA NTA SST is between  $-1$  and  $1$  standard deviations

to a faster transition from the La Niña to the El Niño from the SON season, while the equatorial easterly over the eastern Pacific is weakened in time as the amplitude of NTA cooling is reduced.

In this section, we examined the overall performance of NTA SST in modulating ENSO variability in the CMIP3 and CMIP5 models. There are a few noteworthy points about the similarity between the observations and the MME. The inverse relationship between NTA SST during the boreal spring season and ENSO during the subsequent boreal winter season is simulated successfully in the climate models. The spatial pattern of partial regression (or composite) of SST, precipitation, and low-level wind vector in MME is similar to that of the observations to some extent, indicating that the observed main mechanism in conveying the NTA signal to the Pacific is robust. The fast phase transition of the ENSO due to the NTA SST is also simulated in the MME, to a large extent.

However, there are also considerable differences between the observations and MME. The amplitude of ENSO induced by NTA SST in the MME is systematically weaker than that of the observed. The NTA-induced ENSO is harder to characterize as a WP-type than that in the observation. While this section primarily examined the MME response, next section will investigate inter-model diversity in the NTA-related response, and discuss what causes these disagreements with the observational results.

#### 4 Inter-model differences in the NTA-induced Pacific variability

##### 4.1 Basic states

As shown in Fig. 1, the climate models simulate the strength of the NTA response very differently. In this subsection, we will examine what causes the different strengths

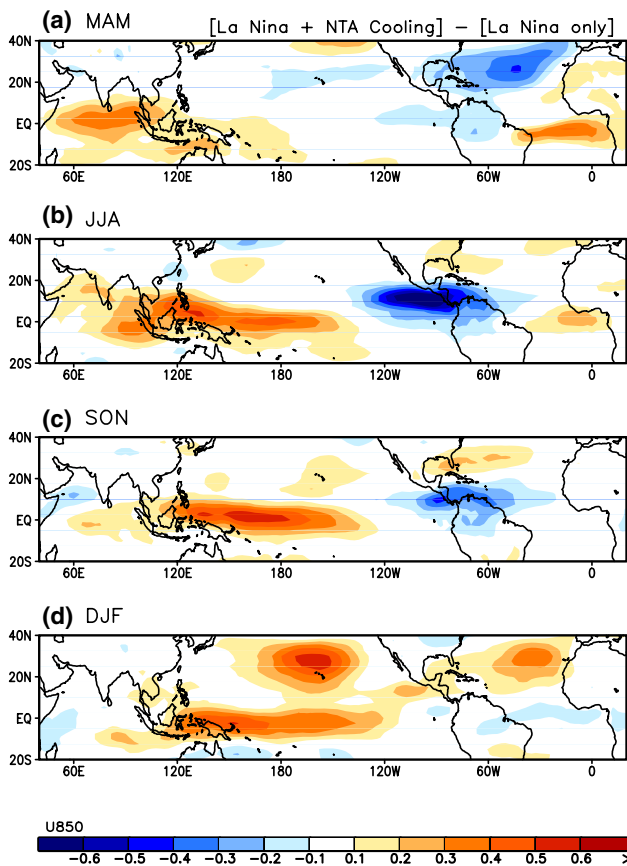


**Fig. 6** Difference in zonal wind at 850 hPa between ‘La Niña + NTA cooling’ and ‘La Niña only’ composite during **a** MAM, **b** JJA, **c** SON, and **d** DJF seasons after the La Niña peak

of the NTA response among the climate models. To quantify the impact of NTA SST on Pacific variability, we use the ‘Strength of the NTA-Effect’ (SNE) index, defined as the partial regression coefficient (Fig. 1). To assess which basic state prefers a stronger NTA response over the Pacific, which tends to be more realistic, we calculated the correlation and regression between the SNE index and seasonal mean basic state, based on the intermodal diversity of the 44 climate models. The correlation/regression pattern indicates an anomalous basic state, defined as a deviation from the MME, which favors a stronger NTA impact.

Figure 7 shows the regression and correlation coefficients of seasonal mean precipitation climatology with the SNE index based on the inter-model diversity. For the FMA season, there is significant positive correlation over the far western off-equatorial Atlantic. This means that wetter basic state over this region is linked to a stronger NTA response (larger SNE index). That is, that NTA warming (cooling) tends to induce a stronger La Niña (El Niño) signal in the subsequent winter season in climate models that have wetter climatology over the western off-equatorial Atlantic during the boreal spring season. This may be

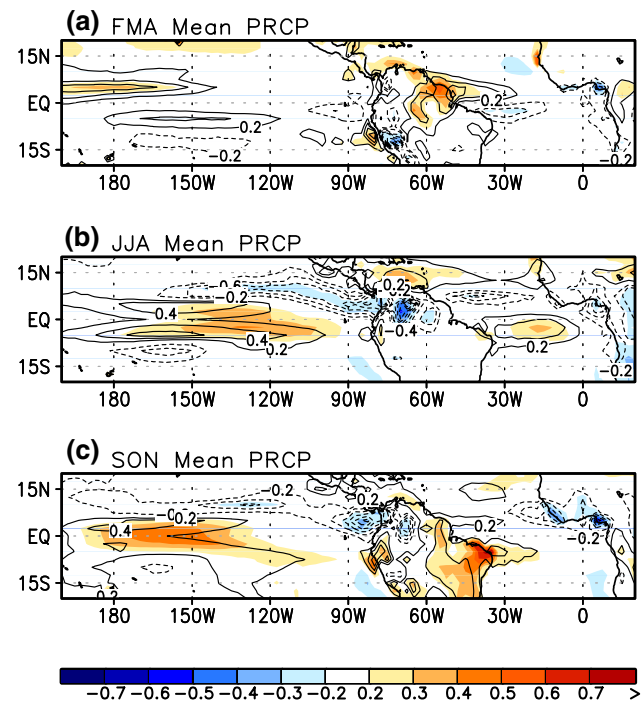


**Fig. 7** The correlation (*shading*), and regression (*contour*) between NTA index and **a** FMA, **b** JJA, and **c** SON mean precipitation

related to the fact that the stronger mean precipitation can provide favorable conditions to generate anomalous convection (Watanabe et al. 2011; Kim et al. 2012; Ham and Kug, 2012; Xiang et al. 2013), while suppressed climatological convection prevents inducing anomalous convection in the response to the SST warming as the anomalous upward motion should overcome the climatological downward motion to lead to the anomalous convective activity. However, when there is climatological upward motion related to the strong convective activity, the SST warming can readily induce the convection anomaly. In this regard, the wetter basic state can lead to stronger local precipitation response to a unit NTA SST anomaly, which can provide a stronger signal to the Pacific sector.

During the JJA season, as the dominant NTA-induced signal appears in the Pacific (Fig. 4b), the mean precipitation over the Pacific becomes important in determining the strength of the NTA response. That is, there is a positive correlation between 150 and 120°W, where there is a significant precipitation anomaly related to the NTA SST (Fig. 4b). This implies that stronger summer-mean precipitation over the central-eastern Pacific tends to intensify the local anomalous precipitation response to enhance the strength of NTA response over the Pacific. This positive correlation signal migrates slightly to the west with time. During the SON season, the mean precipitation between 180 and 150°W becomes most significant in determining

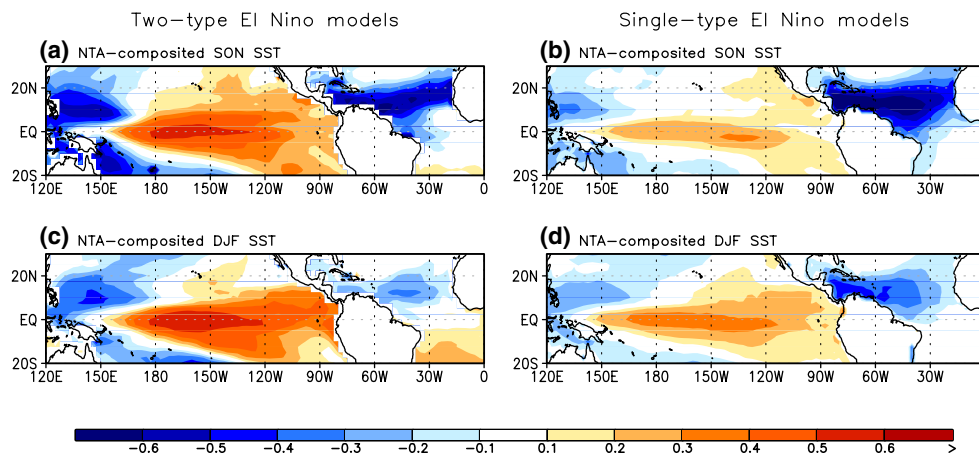


**Fig. 8** Composite of **a** SON, **c** DJF SST after the FMA NTA warming in two-type El Niño models. The *right panel* shows the **b** SON, and **d** DJF SST after the FMA NTA warming in single-type El Niño

models. The single-type, and two-type El Niño models are defined as the highest and lowest correlations between NINO3 and NINO4, respectively

the strength of the NTA response. This is also consistent with the westward shift of NTA-induced convective anomaly from the central-eastern Pacific in the JJA season (Fig. 4b) to the western-central Pacific in the SON season (Fig. 4c). This means that the basic state is crucial for determining the strength of the NTA response, which is closely related to the spatial pattern of NTA SST-induced anomalies.

#### 4.2 Independence between warm-pool and cold-tongue El Niño

Ham et al. (2013a, b) pointed out that the observed NTA-induced ENSO has a SST action center over the central Pacific, while the signal over the eastern Pacific is quite weak. However, the MME result shows that the El Niño induced by NTA SST has an extended SST action center over the central-eastern Pacific. We found that the location of the SST action center induced by NTA SST is dependent on a model's ability to simulate the two types of El Niño independently to some extent. Figure 8 shows the composite of SST after NTA cooling in climate models that simulate one or two types of El Niño events. To measure whether the climate model simulated a single-type or two-type El Niño events, we used correlation between NINO3 and NINO4 during the DJF season, as Ham and Kug (2012) and Kug et al. (2012) did. The low correlation between the two El Niño indices indicates that the model tends to simulate the two types of El Niño events independently, while the models with high correlations tend to simulate mostly single-type El Niño events. We defined the ten climate models that had the lowest correlation between NINO3 and NINO4 as two-type El Niño models, and that with the highest correlation as a single-type El Niño model. Note

that the lowest correlation in the climate models is similar in degree to the correlation in the observation.

For the SON season after the FMA NTA cooling, in the two-type El Niño models, the SST action center induced by NTA SST is located at 180–150°W and the SST signal becomes gradually weaker at the eastern Pacific. On the other hand, the peak SST signal is between 150 and 120°W in the single-type El Niño models, which is shifted to the east, by ~30°, versus that in the two-type El Niño models. This shows that the zonal location of NTA-induced El Niño is dependent on the dependency between two types of El Niño events. This also implies that the model which realistically simulated two types of El Niño events tends to simulate realistic NTA impact to some extent. But, there is no clear difference in the zonal phase of the SST response between two groups during DJF season.

In addition to the zonal location of NTA-induced El Niño, it is also interesting that the amplitude of NTA-induced El Niño in the two-type El Niño models is stronger than that in single-type El Niño models. This may be because the climatology in the two-type El Niño models is wetter than that in the single-type El Niño models. According to Ham and Kug (2012), the two-type El Niño models tend to have wetter climatology over the central-eastern Pacific. They argued that the dry climatological bias with cold SST bias over the central-eastern Pacific confines ENSO-related convective activities to the western Pacific even during CT El Niño events. Therefore, the atmospheric response during the CT El Niño becomes similar to that during the WP El Niño, which means the atmospheric response between the two-types of the El Niño events becomes similar (Jang et al. 2013). Due to the similar atmospheric response, it is more probable to lead stronger coupling between two types of El Niño events.

Consistently, the models with two-type El Niño events tend to simulate wetter climatology (or less climatological dry bias) over the central-eastern Pacific. The differences in the climatological precipitation over the equatorial central-eastern Pacific (i.e., 180–70°W, 5°S–5°N) of two-type El Niño model versus that of the single-type is persistently positive during all seasons. That is, 1.13 mm/day in the JJA season, 0.51 mm/day in the SON season, and 0.90 mm/day in the DJF season. This wetter climatology over the equatorial central-eastern Pacific also tends to enhance the NTA impact (Fig. 7). Thus, the wetter basic state might connect the stronger NTA response to the simulation quality of the two-type El Niño events.

#### 4.3 Phase-locking of ENSO to boreal winter season

In this sub-section, it will be shown that the model performance in simulating phase-locking of the ENSO to the boreal winter season can also lead to the inter-model difference in NTA strength on ENSO variability. The phase-locking of ENSO denotes that the ENSO tends to be at peak phase during the boreal winter season (Tziperman et al. 1998), and we found the simulation quality of the ENSO phase-locking is clearly linked to that of NTA impact on the ENSO in CMIP models. Because the ENSO phase-locking is often measured by the STD of SST at each calendar month (Neelin et al. 2000; Ham and Kug 2012, 2014), Fig. 9 shows the correlation coefficient between STD of Nino4 SST and SNE index for each calendar month using the inter-model diversity of 44 climate models. The positive correlation over the equatorial Pacific means that the strong NTA impact on Pacific variability is linked to the strong variability over the Nino4 region. It is considered that the NTA SST could be an additional source of Pacific SST variability to enhance ENSO variability. Additionally, strong ENSO variability means strong positive feedback processes, which will respond greatly to the same external forcing, such as NTA SST variability.

The interesting point is that there is clear seasonality in the correlation. For example, the correlation between SNE index and STD of Nino4 SST is higher in January and September (i.e., boreal fall or winter seasons), and lower in May and June (boreal summer seasons). This may be because that the main mechanism for NTA SST during the boreal spring season to affect the Pacific SST variability is a slow adjustment process among the SST, wind, and precipitation. That is, once the NTA warming is induced, it takes roughly 3 or 4 months, as shown in Figure 1a of Ham et al. (2013a). Then, the equatorial easterly, related to the anticyclonic flow over the western-central Pacific, induces a La Niña signal, which takes an additional month. Thus, the La Niña signal starts to develop from the boreal fall season.

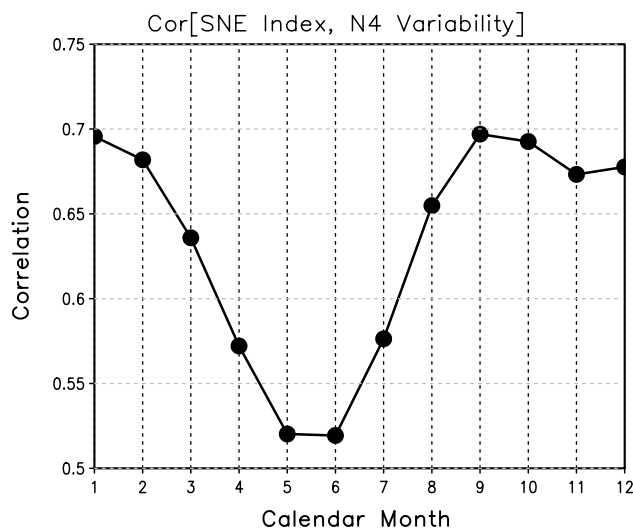


**Fig. 9** The correlation coefficient between standard deviation (STD) of Nino4 SST and SNE index for each calendar month using the inter-model diversity of 44 climate models

Figure 9 is about the relationship within the inter-model (i.e. deviation of each model's result from the MME), which exhibits the model with stronger SNE index tends to have stronger ENSO amplitude than the models with weaker SNE index. The similar explanation can be applied between the observation and MME only when there is no systematic difference except for the NTA impact. However, there are numerous systematic differences between the MME and the observation to determine ENSO amplitude (Kim and Jin 2011), the weaker SNE in the MME does not always guarantee the weaker ENSO amplitude than the observation.

Previous studies have pointed out that current climate models have still systematic problems in simulating the phase-locking of ENSO, and many models simulate the ENSO peak during the boreal summer time, unlike the observational data (Ham and Kug 2012, 2014). If a climate model has an ENSO peak during the boreal summer season (i.e., *unrealistic* ENSO phase-locking), the ENSO variability tends to start decaying from the boreal fall season when the ENSO anomalies due to the NTA SST have to develop. According to Tziperman et al. (1998), the ENSO peak season is when the tropical air-sea coupling is weakest. Also, Ham et al. (2013a, b, c) and Ham and Kug (2014) showed that the CMIP models with summer ENSO peaks tended to have the weakest tropical air-sea coupling strength during the boreal summer season. This implies that the climate models with summer ENSO peaks simulate weak air-sea coupling strength over the tropical Pacific, prohibiting amplification of the NTA-induced signal. On the other hand, in the model with boreal winter ENSO peak (i.e., *realistic* ENSO phase-locking), the ENSO-related coupled feedback

is still relatively strong, until the boreal fall season. Thus, it would act to amplify the NTA-induced ENSO signal. This means that the impact of the NTA SST might be simulated better in models with realistic ENSO phase-locking.

To examine the relationship between NTA index and ENSO phase-locking in more detail, we first define the model's fidelity in simulating ENSO phase-locking. We used the 'Phase-locking Performance (PP) index', suggested by Ham and Kug (2014), which is defined as the correlation between STDs of Nino3 SST anomaly (SSTA) for each model and observation data in each calendar month. They showed that this PP index was consistent with other ENSO phase-locking indexes, as in Bellenger et al. (2013), to examine ENSO phase-locking in climate models. Models with realistic ENSO phase-locking tend to have high PP indexes, while those with summer ENSO peak tends to have lower PP indexes. Using the PP index, we categorized two groups: one comprised the realistic ENSO phase-locking models (or winter ENSO peak models), the ten climate models with highest PP index. Then, the ten climate models with the lowest PP index were defined as the summer ENSO peak models, because the models with low PP indexes tended to have ENSO peaks during the boreal summer season.

Figure 10 shows the partial regression of SST and 850 hPa zonal-wind anomalies on the NTA index in the 'winter ENSO peak models' and the 'summer ENSO peak models.' Note that this figure is same as Fig. 4, except that only the 10 models with highest/lowest PP index are used. During the MAM season, the spatial distributions of NTA warming and 850 hPa zonal-wind are quite similar. During the JJA season, while the 'winter ENSO peak models' exhibit negative SST anomalies over the equatorial Pacific with a low-level easterly, however, the La Niña-related signal is not clear in the 'summer ENSO peak models.' As pointed out in the previous section, the air-sea coupling tends to be weaker during the boreal summer season in the summer ENSO peak models, and it prohibits the growth of the ENSO signal. The differences in the growth of ENSO signal is also clear in the SON and DJF seasons; thus, the negative SST anomalies during the DJF season approach about  $-2$  °C in 'winter ENSO peak models', while it is about  $-0.5$  °C in 'summer ENSO peak models'. This clearly indicates that there is a significant relationship between simulation quality of ENSO phase-locking and the SNE index. It also shows that realistic ENSO phase-locking can be a key factor in simulating realistic NTA responses over the Pacific.

## 5 Summary and conclusions

In this study, the role of NTA SST on ENSO variability in the CMIP3 and CMIP5 simulations is examined. The

inverse relationship between NTA SST during the boreal spring season and the ENSO during the subsequent winter season is well simulated in most of the CMIP models. The partial regression result shows that 42 of the 44 models successfully simulated this inverse relationship. Additionally, westward propagation of the NTA SST-related signal from the Atlantic to the Pacific along the off-equatorial Pacific ITCZ is shown in the MME result, indicating that the main mechanism leading to the inverse relationship between NTA SST and the ENSO is also well simulated in the CMIP models to some extent.

However, there are systematic differences between the observations and the MME results. First, the ENSO triggered by the NTA SST is not WP-type in the MME even if the low-level opposite wind response between the western and eastern Pacific is simulated, as observed. This indicates that the SST over the eastern Pacific is less sensitive to the local wind forcing, while the remote wind forcing over the western Pacific dominates the eastern Pacific SST signal. Additionally, the amplitude of NTA SST-induced ENSO is systematically weaker in the model simulation. Those deficiencies are less obvious in the models that simulate two types of El Niño events, simulating the NTA SST-forced El Niño action center over the central Pacific with stronger amplitude.

In addition to the MME result, inter-model differences in the NTA response were examined. First, we found that the basic state is important in determining the strength of the NTA response over the Pacific. The model with stronger mean precipitation over the western Atlantic during the MAM season provides favorable conditions for the NTA SST to induce a stronger local precipitation anomaly. During the JJA, the mean precipitation over the equatorial central Pacific tends to be linked to the strength of NTA response because this is where the anomalous precipitation due to the NTA SST is robust in this season. It shows that, as the NTA SST-related precipitation anomalies are slowly propagating to the west, the location of mean precipitation, which is directly linked to the strength of the NTA response, is also shifted to the west during the boreal summer and fall seasons.

Second, it was also found that a model with realistic ENSO phase-locking tends to simulate a stronger NTA response. Because it takes several months for the NTA SST during boreal spring season to induce the equatorial wind over the western Pacific, the NTA-induced ENSO SST signal starts to develop from the boreal summer season. In the model with a summer ENSO peak, the decaying mechanism related to the ENSO prevails from the boreal fall season, so that the growth of the NTA-induced ENSO might be weak. However, in a model with a winter ENSO peak, the coupled feedback to amplify the ENSO is still strong up to the boreal winter season, leading to a strong NTA impact in the Pacific.

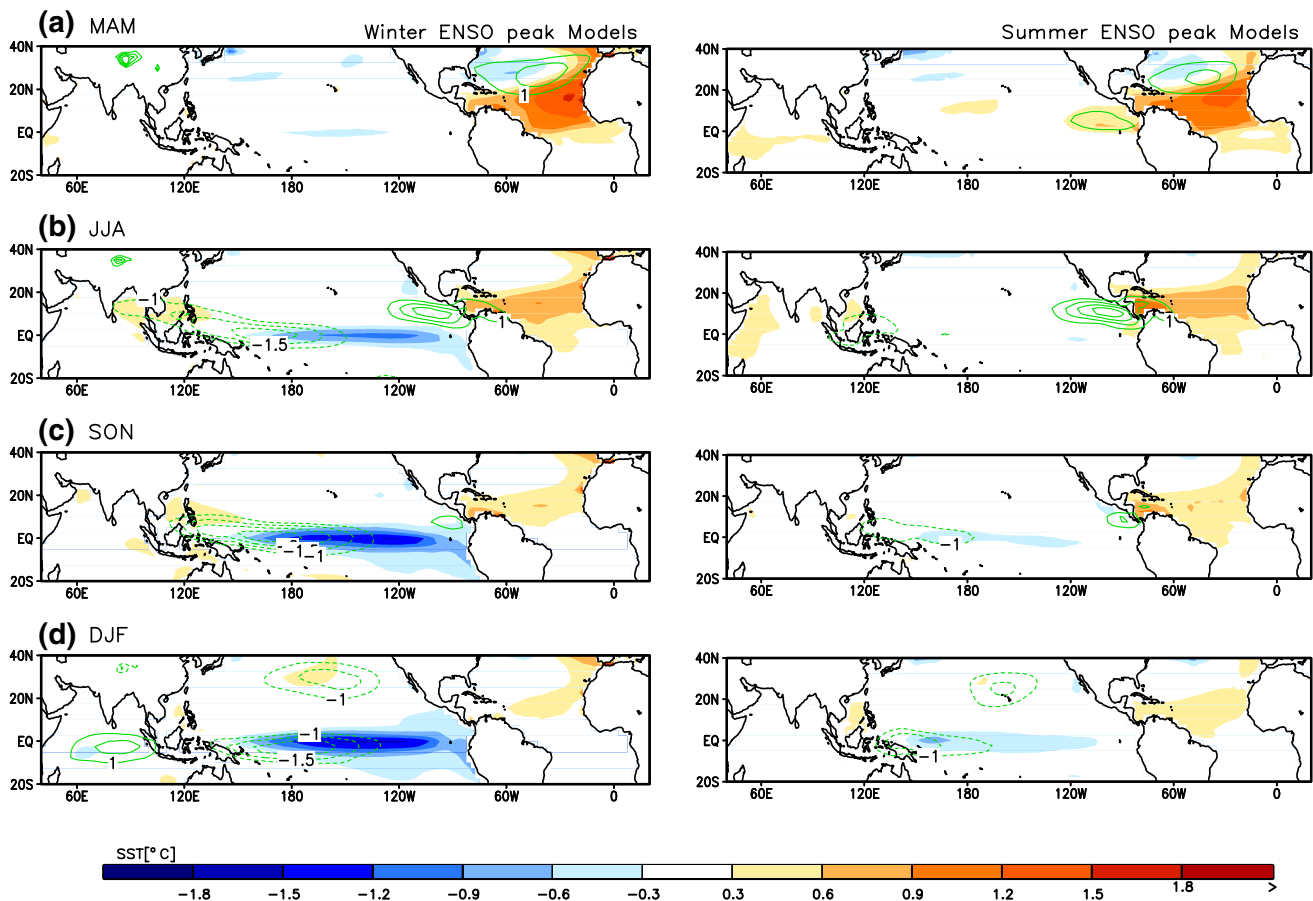


**Fig. 10** The partial regression of SST, precipitation, and wind vector at 850 hPa during the **a** MAM, **b** JJA, **c** SON, and **d** DJF seasons on the FMA NTA SST after excluding the impact of NINO3.4 during

the previous DJF season in ‘winter ENSO peak models or highest PP-index models’ (*left panels*), and ‘summer ENSO peak models or lowest PP-index models’ (*right panels*)

This study examines the overall response over the Pacific due to the NTA SST in the CMIP models. We showed that the CMIP models have the ability to simulate NTA SST-related signals over the Pacific to some extent. These findings indicate that the current state-of-the-art models can be powerful tools for examining the inter-basin relationship in more detail, including the decadal modulation of the relationship between NTA SST and ENSO, changes in the inter-basin relationship after global warming, the asymmetry of NTA strength on Pacific variability between NTA cooling and warming (Fig. 2), and the impact of inter-basin relationships on ENSO forecasting. Further studies will provide a foundation to extend the ENSO dynamics and theories outside the Pacific basin, and increase our understanding about the equatorial atmosphere-oceanic coupled dynamics.

**Acknowledgments** This work was supported by National Research Foundation (NRF- 2014R1A2A2A01003827).

## References

- Alexander M, Scott J (2002) The influence of ENSO on air-sea interaction in the Atlantic. *Geophys Res Lett* 29:46-1–46-4
- An S-I, Jin F-F (2004) Nonlinearity and asymmetry of ENSO. *J Clim* 17:2399–2412
- Ashok K, Behera SK, Rao SA, Weng H, Yamagata T (2007) El Niño Modoki and its possible teleconnection. *J Geophys Res* 112:C11007. doi:10.1029/2006JC003798
- Burger G, Stephenson DB (1999) The “normality” of El Niño. *Geophys Res Lett* 26(8):1027–1030
- Chiang JC, Sobel AH (2002) Tropical tropospheric temperature variations caused by ENSO and their influence on the remote tropical climate. *J Clim* 15:2616–2631
- Covey DL, Hastenrath S (1978) The Pacific El Niño phenomenon in the Atlantic sector. *Mon Weather Rev* 106:1280–1287
- Curtis S, Hastenrath S (1995) Forcing of anomalous sea surface temperature evolution in the tropical Atlantic during Pacific warm events. *J Geophys Res* 100:15835–15847
- Ding H, Keenlyside NS, Latif M (2012) Impact of the equatorial atlantic on the El Niño Southern Oscillation. *Clim Dyn* 38:1965–1972
- Dommenget D, Semenov V, Latif M (2006) Impacts of the tropical Indian and Atlantic Oceans on ENSO. *Geophys Res Lett* 33:L11701. doi:10.1029/2006GL025871

- Dong B, Sutton RT, Scaife AA (2006) Multidecadal modulation of El Niño–Southern Oscillation (ENSO) variance by Atlantic Ocean sea surface temperatures. *Geophys Res Lett* 33
- Enfield DB, Mayer DA (1997) Tropical Atlantic sea surface temperature variability and its relation to El Niño–Southern Oscillation. *J Geophys Res* 102:929–945
- Frauen C, Dommenges D (2012) Influences of the tropical Indian and Atlantic Oceans on the predictability of ENSO. *Geophys Res Lett* 39:L02706
- Ham Y-G, Kug J-S (2012) How well do current climate models simulate two types of El Niño? *Clim Dyn* 39:383–398
- Ham Y-G, Kug J-S (2014) ENSO phase-locking to the boreal winter in CMIP3 and CMIP5 models. *Clim Dyn*. doi:10.1007/s00382-014-2064-1
- Ham Y-G, Kug J-S, Park J-Y, Jin F-F (2013a) Sea surface temperature in the north tropical Atlantic as a trigger for El Niño/Southern Oscillation events. *Nat Geosci* 6:112–116
- Ham Y-G, Kug J-S, Park J-Y (2013b) Two distinct roles of Atlantic SSTs in ENSO variability: north Tropical Atlantic SST and Atlantic Niño. *Geophys Res Lett* 40:4012–4017
- Ham Y-G, Kug J-S, Kim D, Kim Y-H, Kim D-H (2013c) What controls phase-locking of ENSO to boreal winter in coupled GCMs? *Clim Dyn* 40:1551–1568
- Hendon HH, Lim E, Wang G, Alves O, Hudson D (2009) Prospects for predicting two flavors of El Niño. *Geophys Res Lett* 36:L19713. doi:10.1029/2009GL040100
- Illig S, Dewitte B (2006) Local coupled equatorial variability versus remote ENSO forcing in an intermediate coupled model of the tropical Atlantic. *J Clim* 19:5227–5252. doi:10.1175/JCLI3922.1
- Izumo T et al (2010) Influence of the state of the Indian Ocean Dipole on the following year's El Niño. *Nat Geosci* 3(3):168–172
- Jang Y-S, Kim D, Kim Y-H, Kim D-H, Watanabe M, Jin F-F, Kug J-S (2013) Simulation of two types of El Niño from different convective parameters. *Asia-Pac J Atmos Sci* 49:193–199
- Jansen MF, Dommenges D, Keenlyside NS (2009) Tropical atmosphere–ocean interactions in a conceptual framework. *J Clim* 22:550–567
- Jeong H-I, Lee DY, Ashok K, Ahn J-B, Lee J-Y, Luo J-J, Schemm J-KE, Hendon HH, Braganza K, Ham Y-G (2012) Assessment of the APCC coupled MME suite in predicting the distinctive climate impacts of two flavors of ENSO during boreal winter. *Clim Dyn* 39:475–493. doi:10.1007/s00382-012-1359-3
- Jin F-F (1997) An equatorial Ocean recharge paradigm for ENSO. Part I: conceptual model. *J Atmos Sci* 54:811–829
- Joseph R, Nigam S (2006) ENSO evolution and teleconnections in IPCCs twentieth-century climate simulations: realistic representation? *J Clim* 19:4360–4377
- Kao H-Y, Yu J-Y (2009) Contrasting eastern-Pacific and central-Pacific types of ENSO. *J Clim* 22:615–632. doi:10.1175/2008-JCLI2309.1
- Keenlyside NS, Latif M (2007) Understanding equatorial Atlantic interannual variability. *J Clim* 20:131–142
- Kim ST, Jin F-F (2011) An ENSO stability analysis. Part II: results from the twentieth and twenty-first century simulations of the CMIP3 models. *Clim Dyn* 36:1609–1627
- Klein SA, Soden BJ, Lau NC (1999) Remote sea surface temperature variations during ENSO: evidence for a tropical atmospheric bridge. *J Clim* 12(4):917–932
- Kug J-S, Kang S-I (2006) Interactive feedback between ENSO and the Indian Ocean. *J clim* 19(9):1784–1801
- Kug J-S, An S-I, Jin F-F, Kang I-S (2005) Preconditions for El Niño and La Niña onsets and their relation to the Indian Ocean. *Geophys Res Lett* 32:L05706. doi:10.1029/2004GL021674
- Kug J-S, Jin F-F, An S-I (2009) Two types of El Niño events: cold tongue El Niño and warm pool El Niño. *J Clim* 22
- Kug J-S, Ham Y-G, Lee J-Y, Jin F-F (2012) Improved simulation of two types of El Niño in CMIP5 models. *Environ Res Lett* 7:034002
- Merle J, Fieux M, Hisard P (1980) Annual signal and interannual anomalies of sea surface temperature in the eastern equatorial Atlantic Ocean. *Deep Sea Res* 26:77–101
- Neelin JD, Jin F-F, Syu H-H (2000) Variations in ENSO phase locking. *J Clim* 13:2570–2590
- Ohba M, Watanabe M (2012) Role of the Indo-Pacific interbasin coupling in predicting asymmetric ENSO transition and duration. *J Clim* 25:9
- Rienecker MM, Suarez MJ, Gelaro R, Todling R, Bacmeister J, Liu E, Bosilovich MG, Schubert SD, Takacs L, Kim G-K (2011) MERRA: NASA's modern-era retrospective analysis for research and applications. *J Clim* 24(14):3624–3648
- Rodríguez-Fonseca B, Polo I, García-Serrano J, Losada T, Mohino E, Mechoso CR, Kucharski F (2009) Are Atlantic Niños enhancing Pacific ENSO events in recent decades? *Geophys Res Lett* 36:L20705
- Saravanan R, Chang P (2000) Interaction between tropical Atlantic variability and El Niño–Southern Oscillation. *J Clim* 13:2177–2194
- Servain J, Picaut J, Merle J (1982) Evidence of remote forcing in the equatorial Atlantic Ocean. *J Phys Oceanogr* 12:457–463
- Smith TM, Reynolds RW, Peterson TC, Lawrimore J (2008) Improvements to NOAA's historical merged land–ocean surface temperature analysis (1880–2006). *J Clim* 21:2283–2296
- Su J, Zhang R, Li T, Rong X, Kug J-S, Hong C-C (2010) Causes of the El Niño and La Niña amplitude asymmetry in the equatorial Eastern Pacific. *J Clim* 23:605–617
- Tziperman E, Cane MA, Zebiak SE, Xue Y, Blumenthal B (1998) Locking of El Niño's peak time to the end of the calendar year in the delayed oscillator picture of ENSO. *J Clim* 11:2191–2203
- Watanabe M, Chikira M, Imada Y, Kimoto M (2011) Convective control of ENSO simulated in MIROC. *J Clim* 24(2):543–562
- Wu R, Kirtman BP (2004) Understanding the impacts of the Indian Ocean on ENSO variability in a coupled GCM. *J Clim* 17(20):4019–4031
- Xiang B, Wang B, Yu W, Xu S (2013) How can anomalous western north Pacific subtropical high intensify in late summer? *Geophys Res Lett* 40(10):2349–2354
- Yeh S-W, Kug J-S, An S-I (2014) Recent progress on two types of El Niño: observations, dynamics, and future changes. *Asia-Pac J* 50:69–81